Motion of a rotatory molecular motor and the chemical reaction rate

Hiroshi Miki, Masatoshi Sato, and Mahito Kohmoto
The Institute for Solid State Physics, The University of Tokyo, 5-1-5 Kashiwanoha, Kashiwa, Chiba 277-8581, Japan
(Received 9 June 2003; published 18 December 2003)

We examine the dependence of the physical quantities of the rotatory molecular motor, such as the rotation velocity and the proton translocation rate, on the chemical reaction rate using the model based only on diffusion process. A peculiar behavior of proton translocation is found and the energy transduction efficiency of the motor protein is enhanced by this behavior. We give a natural explanation that this behavior is universal when certain inequalities between chemical reaction rates hold. That may give a clue to examine whether the motion of the molecular motor is dominated by diffusion process or not.

DOI: 10.1103/PhysRevE.68.061906 PACS number(s): 87.15.−v, 05.40.−a, 05.60.−k

I. INTRODUCTION

Many kinds of molecular motors are known to play essential roles of life. The word ''molecular motor'' is, in a wide sense, used to describe protein molecules that transduce chemical energy from some source into mechanical work (and in some case, vice versa). Molecular motors are classified into two kinds: linear and rotatory motors. As the former, myosins, kinesins, and dyneins, which slide along the specific filaments in the specific direction, respectively, are known to work for muscle construction, transport of materials in cell, etc. by hydrolyzing adenosine triphosphate (ATP) [1,2]. As the latter, two motors are known to date. One is bacteria flagellar motor, which works as a propeller by gaining chemical energy from the proton gradient across the membrane. The other is ATP synthase which is found in membranes of living things. It works wholly as a transducer between the energy of proton gradient across the membrane and that of ATP synthesis from adenosine diphosphate (ADP) and inorganic phosphate. It can both synthesize ATP and pump proton against the proton gradient by hydrolyzing ATP (see Figs. 16.28 in Ref. [3]). It is composed of two parts, the F_o part and the F_1 part, each is known to work as a rotatory motor [4–17]. The F_o part is embedded in the membrane. It contains a proton channel and transduces the energy of transmembrane proton gradient into rotatory torque when working as synthesizer. The F_1 part plays a role of ATP synthesis/hydrolysis, transducing rotatory torque into the energy required for ATP synthesis and vice versa.

It is believed generally that the energy transduction efficiency of molecular motor, that is, the ratio of the energy output to input from the energy source, is extremely high. For example, it is reported in Ref. [12] that the efficiency is almost 100% for the F_1 part of ATP synthase. Thus, understanding the mechanism of molecular motors, especially that of energy transduction, is important not only because of their many roles of life, but also because of the possibility that, if this mechanism is novel, it may be applied to a new technology as a machine with high energy transduction efficiency, even if it can be used only in a constrained scale. In the scale of motor molecule (~10–100 nm), water molecules collide with motor molecules many times. These collisions make the diffusive motion of the motor molecule and thus it is natural to infer that this collision effect contributes to the motion of motor, but there is no crucial evidence that it is essential.

Here we take up a simple model inspired by the F_o part of ATP synthase [19,20] and examine the dependence of the rotation velocity and the proton translocation rate of this model on the chemical reaction rates. The efficiency of energy transduction is calculated from these quantities. As far as we know, there is no computation of this kind.

II. MODEL

The F_o part is schematically drawn in Figs. 1 and 2. It contains three types of subunits, *a*, *b*, and *c*. As shown in Fig. 1, the *a* subunit is fixed in the membrane. The *b* subunit connects the F_o and F_1 parts but it is not shown in Figs. 1 and 2 (see Ref. [3]). The *c* subunits are arranged in a ring and this ring rotates accompanying the proton translocation.

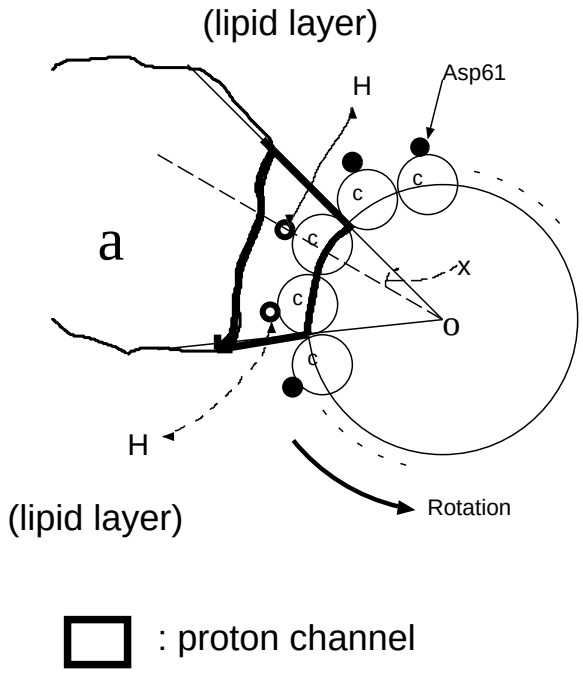

FIG. 1. The proton channel viewed from the basic side, the inner side of the membrane. There are the *c* subunits arranged in a ring and the ring rotates counterclockwise during synthesis. The position variable *x* is defined as a rotation angle of the ring.

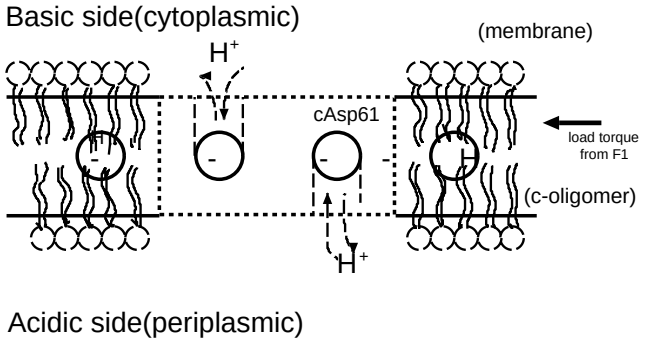

FIG. 2. The proton channel viewed from the *a* subunit. There are two proton binding sites in the channel and only these two can be either protonated or unprotonated. The left path of protons is from the basic side and the right path is from the acidic side [5]. These proton binding sites move rightward during synthesis despite the leftward load from the F_1 part.

There is a proton binding site in almost the middle of each *c* subunit, Asp61, a carboxyrate. A proton passes through the interface between the *a* and *c* subunits (but as described later, not directly), called proton channel. In the proton channel, there are two paths to these binding sites, the left one is from the basic side, the inner side of the membrane, and the right is from the acidic side, the outer one (see Fig. 2) [5]. Proton concentration in the acidic side is kept higher than that in the basic side by respiratory chains, which pumps protons in the basic side out of the membrane. Roughly speaking, a proton flows into and binds to the right site from acidic side, goes through the membrane with *c*-ring rotation, and dissociates from the left site and flows out to the basic side. That is, a proton passes through the proton channel not directly but via the membrane accompanying the rotation of the *c* ring.

We investigate the above situation using the ''(simply) biased diffusion model'' [19,20]. It was first presented to explain the rotation of bacteria flagellar motor which has similar structure to the F_o part of the ATP synthase but is one order larger in linear dimension. The mechanism is as follows: There are N proton binding sites in the rotor (i.e., the ring is composed of N *c* subunits and $N=9-12$ in *Escherichia coli*) at same intervals and two of them are in the proton channel. Only two proton binding sites are allowed to be in the channel and each of them can be protonated or unprotonated. The others can be only protonated due to the hydrophobicity of the membrane. Thus the states of the motor are determined by the protonation of the two proton binding sites in the channel: E is the empty state where both sites are unprotonated, R is the right state where the right site is protonated and the left is unprotonated, L is the left state where the left site is protonated and the right is unprotonated, and F is the full state where both sites are protonated. We assume that a proton does not hop between two proton binding sites. When one of the proton binding sites in the channel comes to the boundary, it can move into the membrane only if it is protonated and otherwise cannot move due to hydrophobicity of the membrane. If there is difference from detailed balance between the rates of one site at which a proton binds to or dissociates from it and those of the other due to the transmembrane proton gradient, it become possible to take out a net motion.

Dynamics of each state is described by the Langevin equation

$$\frac{dx}{dt} = -\gamma_i \frac{d\phi_i(x)}{dx} + R_i(t), \tag{1}$$

where i refers to the state, γ_i is the friction constant, and x is the position of the motor (see Fig. 1) which is explicitly defined later. The potential $\phi_i(x)$ represents the load torque τ from the F_1 part, so $\phi_i(x)=\tau x$ [12]. $R_i(t)$ is the random force of Gaussian noise, which satisfies

$$\langle R_i(t)\rangle = 0, \tag{2}$$

$$\langle R_i(t)R_j(t')\rangle = 2D_i\delta_{ij}\delta(t-t'), \tag{3}$$

where $\langle\cdots\rangle$ is the time average and D_i is the diffusion constant satisfying the Einstein's relation, $D_i=\gamma_i k_B T$ (T, temperature; k_B, the Boltzmann constant). The constants D_i and γ_i depend on the states since the different conformations have different surface areas, densities, etc. But for simplicity, it is assumed below that all the states have effectively the same values, $\gamma_i=\gamma$ and $D_i=D$, since those differences are small. In addition to the above single-state motions, transitions between different states occur. Thus it is convenient to adopt the formulation of the Fokker-Planck equation equivalent to Eq. (1),

$$\frac{\partial}{\partial t}\mathbf{p}(x,t) = -\frac{\partial}{\partial x}\mathbf{\Pi}(x,t) + \hat{\mathbf{K}}(x)\cdot\mathbf{p}(x,t), \tag{4}$$

$$\mathbf{\Pi}(x,t) = \gamma\hat{\mathbf{f}}(x)\mathbf{p}(x,t) - D\frac{\partial}{\partial x}\mathbf{p}(x,t), \tag{5}$$

where $\hat{\mathbf{f}}$ is the external force $\hat{\mathbf{f}}=\mathrm{diag}[\tau,\tau,\ldots,\tau]$ and $\hat{\mathbf{K}}$ is the transition matrix which describes changes between states. The system discussed here has four-component probability $\mathbf{p}(x,t)$ and flow $\mathbf{\Pi}(x,t)$:

$$\mathbf{p}(x,t) = \begin{bmatrix} p_E(x,t) \\ p_R(x,t) \\ p_L(x,t) \\ p_F(x,t) \end{bmatrix}, \quad \mathbf{\Pi}(x,t) = \begin{bmatrix} \Pi_E(x,t) \\ \Pi_R(x,t) \\ \Pi_L(x,t) \\ \Pi_F(x,t) \end{bmatrix}, \tag{6}$$

where $p_i(x,t)$ and $\Pi_i(x,t)$ $(i=E,R,L,F)$ describe the probability and its flow that the motor in state i is at position x and at time t. The coordinate x is placed as follows: The origin O is set at the center of the *c* ring and the position variable x is defined as a rotation angle (Fig. 1). The proton channel extends from $x=0$ to δ ($\delta=2\pi/N$ and $N=12$ fixed hereafter). $x=0$ is the position that the left proton binding site is at the left boundary of the channel, and $x=\delta$ is the position that the right site is at the right boundary. When one site moves into the membrane, another site appears into the channel from the other side of the membrane. In this sense,

the system has periodicity. These constraints of periodicity and hydrophobicity mentioned above are expressed by imposing the boundary conditions on Eq. (4),

$$\Pi_E(0,t)=\Pi_E(\delta,t)=0, \tag{7}$$

$$\Pi_R(0,t)=\Pi_L(\delta,t)=0, \tag{8}$$

$$\Pi_L(0,t)=\Pi_R(\delta,t), \tag{9}$$

and

$$\Pi_F(0,t)=\Pi_F(\delta,t). \tag{10}$$

The transition rate matrix is written as

$$\hat{\mathbf{K}}=\begin{bmatrix} -(k_{in}^R+k_{in}^L) & k_{out}^R & k_{out}^L & 0 \\ k_{in}^R & -(k_{out}^R+k_{in}^L) & 0 & k_{out}^L \\ k_{in}^L & 0 & -(k_{in}^R+k_{in}^L) & k_{out}^R \\ 0 & k_{in}^L & k_{in}^R & -(k_{out}^R+k_{out}^L) \end{bmatrix}. \tag{11}$$

There are a few assumptions in the above expression of the transition rate matrix:

(1) The chemical reaction, that is, binding and/or dissociation of proton to/from the sites, is sufficiently fast compared with the motion of the motor protein. This is justified because the mass and size of a proton is much smaller than those of the motor so the diffusion coefficient of a proton is much larger than that of the motor protein.

(2) There is no correlation between the reaction of the left site and that of the right site.

(3) The reaction rates are independent of the position of the motor x. This assumption may have to be modified to take account of other influences, for instance, interaction between residues [19]. But we neglect the influences like these for simplicity.

In this case, for example, it is thought that k_{ER}, the rate at which state E switches to state R, and k_{LF}, the one at which L switches to F, are both written by k_{in}^R, the one at which a proton binds to the empty right site. So, similarly we set

$$k_{ER}=k_{LF}=k_{in}^R, \tag{12}$$

$$k_{EL}=k_{RF}=k_{in}^L, \tag{13}$$

$$k_{RE}=k_{FL}=k_{out}^R, \tag{14}$$

and

$$k_{LE}=k_{FR}=k_{out}^L. \tag{15}$$

For the motor to work, the detailed balance should be violated due to the free energy acquired from a proton passage of the channel, ΔG. Thus the ratio of transition rate from L to R via E or F to that from R to L is written as

$$\frac{(L\to R)}{(R\to L)}=\frac{k_{LE}k_{ER}+k_{LF}k_{FR}}{k_{RE}k_{EL}+k_{RF}k_{FL}}=\frac{k_{in}^R k_{out}^L}{k_{in}^L k_{out}^R}=\exp[\Delta G/k_B T], \tag{16}$$

where ΔG is a function of ΔpH ($\Delta pH=pH_B-pHs_A$, A and B denote the acidic and basic sides, respectively), and V the membrane potential accompanying this difference of proton concentration and written as

$$\Delta G=V+k_B T\ln[10^{\Delta pH}]. \tag{17}$$

Under these assumptions, this model can be solved analytically. The transition rate matrix $\hat{\mathbf{K}}$ is diagonalized by the matrix $\hat{\mathbf{Q}}$:

$$\hat{\mathbf{Q}}=\begin{bmatrix} k_{out}^R k_{out}^L & -k_{out}^R & -k_{out}^L & 1 \\ k_{in}^R k_{out}^L & -k_{in}^R & k_{out}^L & -1 \\ k_{out}^R k_{in}^L & k_{out}^R & -k_{in}^L & -1 \\ k_{in}^R k_{in}^L & k_{in}^R & k_{in}^L & 1 \end{bmatrix}, \tag{18}$$

$$\hat{\mathbf{Q}}^{-1}=\frac{1}{(k_{in}^L+k_{out}^L)(k_{in}^R+k_{out}^R)} \times\begin{bmatrix} 1 & 1 & 1 & 1 \\ -k_{in}^L & -k_{in}^L & k_{out}^L & k_{out}^L \\ -k_{in}^R & k_{out}^R & -k_{in}^R & k_{out}^R \\ k_{in}^L k_{in}^R & -k_{in}^L k_{out}^R & -k_{out}^L k_{in}^R & k_{out}^L k_{out}^R \end{bmatrix}, \tag{19}$$

and

$$\hat{\mathbf{Q}}^{-1}\hat{\mathbf{K}}\hat{\mathbf{Q}}=\begin{bmatrix} 0 & & & \\ & -(k_{\mathrm{in}}^{\mathrm{L}}+k_{\mathrm{out}}^{\mathrm{L}}) & & \\ & & -(k_{\mathrm{in}}^{\mathrm{R}}+k_{\mathrm{out}}^{\mathrm{R}}) & \\ & & & -(k_{\mathrm{in}}^{\mathrm{R}}+k_{\mathrm{in}}^{\mathrm{L}}+k_{\mathrm{out}}^{\mathrm{R}}+k_{\mathrm{out}}^{\mathrm{L}}) \end{bmatrix}. \tag{20}$$

Then in a steady state, Eq. (4) is reduced to

$$0=-\frac{d}{dx}\left[\gamma\tau-D\frac{d}{dx}\right](\hat{\mathbf{Q}}^{-1}\mathbf{p}(x))+\begin{bmatrix} 0 & & & \\ & -(k_{\mathrm{in}}^{\mathrm{L}}+k_{\mathrm{out}}^{\mathrm{L}}) & & \\ & & -(k_{\mathrm{in}}^{\mathrm{R}}+k_{\mathrm{out}}^{\mathrm{R}}) & \\ & & & -(k_{\mathrm{in}}^{\mathrm{R}}+k_{\mathrm{in}}^{\mathrm{L}}+k_{\mathrm{out}}^{\mathrm{R}}+k_{\mathrm{out}}^{\mathrm{L}}) \end{bmatrix}(\hat{\mathbf{Q}}^{-1}\mathbf{p}(x)). \tag{21}$$

The solution of Eq. (21) is

$$(\hat{\mathbf{Q}}^{-1}\mathbf{p}(x))=\begin{bmatrix} C_1+C_2e^{\xi x} \\ C_3e^{\eta_{\mathrm{L}}^{+}x}+C_4e^{\eta_{\mathrm{L}}^{-}x} \\ C_5e^{\eta_{\mathrm{R}}^{+}x}+C_6e^{\eta_{\mathrm{R}}^{-}x} \\ C_7e^{\eta_{\mathrm{LR}}^{+}x}+C_8e^{\eta_{\mathrm{LR}}^{-}x} \end{bmatrix}, \tag{22}$$

where C_i $(i=1,2,\ldots,8)$ are integral constants and

$$\xi=\frac{\gamma\tau}{D}, \tag{23}$$

$$\eta_{\mathrm{L}}^{\pm}=\frac{\gamma\tau\pm\sqrt{(\gamma\tau)^2+4D(k_{\mathrm{in}}^{\mathrm{L}}+k_{\mathrm{out}}^{\mathrm{L}})}}{2D}, \tag{24}$$

$$\eta_{\mathrm{R}}^{\pm}=\frac{\gamma\tau\pm\sqrt{(\gamma\tau)^2+4D(k_{\mathrm{in}}^{\mathrm{R}}+k_{\mathrm{out}}^{\mathrm{R}})}}{2D}, \tag{25}$$

and

$$\eta_{\mathrm{LR}}^{\pm}=\frac{\gamma\tau\pm\sqrt{(\gamma\tau)^2+4D(k_{\mathrm{in}}^{\mathrm{L}}+k_{\mathrm{out}}^{\mathrm{L}}+k_{\mathrm{in}}^{\mathrm{R}}+k_{\mathrm{out}}^{\mathrm{R}})}}{2D}. \tag{26}$$

Therefore, we obtain

$$\mathbf{p}(x)=\hat{\mathbf{Q}}(\hat{\mathbf{Q}}^{-1}\mathbf{p}(x))=\begin{bmatrix} k_{\mathrm{out}}^{\mathrm{R}}k_{\mathrm{out}}^{\mathrm{L}}(C_1+C_2e^{\xi x})-k_{\mathrm{out}}^{\mathrm{R}}(C_3e^{\eta_{\mathrm{L}}^{+}x}+C_4e^{\eta_{\mathrm{L}}^{-}x})-k_{\mathrm{out}}^{\mathrm{L}}(C_5e^{\eta_{\mathrm{R}}^{+}x}+C_6e^{\eta_{\mathrm{R}}^{-}x})+C_7e^{\eta_{\mathrm{LR}}^{+}x}+C_8e^{\eta_{\mathrm{LR}}^{-}x} \\ k_{\mathrm{in}}^{\mathrm{R}}k_{\mathrm{out}}^{\mathrm{L}}(C_1+C_2e^{\xi x})-k_{\mathrm{in}}^{\mathrm{R}}(C_3e^{\eta_{\mathrm{L}}^{+}x}+C_4e^{\eta_{\mathrm{L}}^{-}x})+k_{\mathrm{out}}^{\mathrm{L}}(C_5e^{\eta_{\mathrm{R}}^{+}x}+C_6e^{\eta_{\mathrm{R}}^{-}x})-C_7e^{\eta_{\mathrm{LR}}^{+}x}-C_8e^{\eta_{\mathrm{LR}}^{-}x} \\ k_{\mathrm{out}}^{\mathrm{R}}k_{\mathrm{in}}^{\mathrm{L}}(C_1+C_2e^{\xi x})+k_{\mathrm{out}}^{\mathrm{R}}(C_3e^{\eta_{\mathrm{L}}^{+}x}+C_4e^{\eta_{\mathrm{L}}^{-}x})-k_{\mathrm{in}}^{\mathrm{L}}(C_5e^{\eta_{\mathrm{R}}^{+}x}+C_6e^{\eta_{\mathrm{R}}^{-}x})-C_7e^{\eta_{\mathrm{LR}}^{+}x}-C_8e^{\eta_{\mathrm{LR}}^{-}x} \\ k_{\mathrm{in}}^{\mathrm{R}}k_{\mathrm{in}}^{\mathrm{L}}(C_1+C_2e^{\xi x})+k_{\mathrm{in}}^{\mathrm{R}}(C_3e^{\eta_{\mathrm{L}}^{+}x}+C_4e^{\eta_{\mathrm{L}}^{-}x})+k_{\mathrm{in}}^{\mathrm{L}}(C_5e^{\eta_{\mathrm{R}}^{+}x}+C_6e^{\eta_{\mathrm{R}}^{-}x})+C_7e^{\eta_{\mathrm{LR}}^{+}x}+C_8e^{\eta_{\mathrm{LR}}^{-}x} \end{bmatrix}, \tag{27}$$

and

$$\mathbf{\Pi}(x)=\hat{\mathbf{Q}}\left[\gamma\tau-D\frac{d}{dx}\right](\hat{\mathbf{Q}}^{-1}\mathbf{p}(x)) =\hat{\mathbf{Q}}\begin{bmatrix} C_1\gamma\tau \\ C_3D\eta_{\mathrm{L}}^{-}e^{\eta_{\mathrm{L}}^{+}x}+C_4D\eta_{\mathrm{L}}^{+}e^{\eta_{\mathrm{L}}^{-}x} \\ C_5D\eta_{\mathrm{R}}^{-}e^{\eta_{\mathrm{R}}^{+}x}+C_6D\eta_{\mathrm{R}}^{+}e^{\eta_{\mathrm{R}}^{-}x} \\ C_7D\eta_{\mathrm{LR}}^{-}e^{\eta_{\mathrm{LR}}^{+}x}+C_8D\eta_{\mathrm{LR}}^{-}e^{\eta_{\mathrm{LR}}^{-}x} \end{bmatrix}. \tag{28}$$

The integral constants C_i's are determined to satisfy the boundary conditions (7)–(10). Five of these six boundary conditions are independent but the rest one is not because from Eq. (4), the following relation is always satisfied in the steady state:

$$\begin{aligned} 0&=\frac{\partial}{\partial t}\int_0^{\delta}dx\sum_i p_i(x,t) \\ &=-\int_0^{\delta}dx\sum_i\frac{\partial}{\partial x}\Pi_i(x,t) \\ &=\sum_i[\Pi_i(0,t)-\Pi_i(\delta,t)]. \end{aligned} \tag{29}$$

In addition to these boundary conditions, the periodicity of the probability at the boundaries

$$p_{\mathrm{R}}(\delta)=p_{\mathrm{L}}(0), \tag{30}$$

$$p_{\mathrm{F}}(\delta)=p_{\mathrm{F}}(0), \tag{31}$$

and the normalization condition

$$\int_0^{\delta} dx \sum_i p_i(x)=1 \tag{32}$$

are necessary in order to close the equations for C_i's. Using these conditions C_i's are determined as

$$\mathbf{c}=\hat{\mathbf{M}}^{-1}\mathbf{s}, \tag{33}$$

where

$$\mathbf{c}=\begin{bmatrix} C_1 \\ C_2 \\ \vdots \\ C_8 \end{bmatrix}, \tag{34}$$

$$\mathbf{s}=\frac{1}{(k_{\mathrm{in}}^{\mathrm{L}}+k_{\mathrm{out}}^{\mathrm{L}})(k_{\mathrm{in}}^{\mathrm{R}}+k_{\mathrm{out}}^{\mathrm{R}})}\begin{bmatrix} 0 \\ 0 \\ \vdots \\ 1 \end{bmatrix}, \tag{35}$$

and

$$\hat{\mathbf{M}}=\begin{bmatrix}
k_{\mathrm{in}}^{\mathrm{R}}k_{\mathrm{out}}^{\mathrm{L}}\gamma\tau & 0 & -k_{\mathrm{in}}^{\mathrm{R}}D\eta_{\mathrm{L}}^{-} & -k_{\mathrm{in}}^{\mathrm{R}}D\eta_{\mathrm{L}}^{+} \\
k_{\mathrm{out}}^{\mathrm{R}}k_{\mathrm{in}}^{L}\gamma\tau & 0 & k_{\mathrm{out}}^{\mathrm{R}}D\eta_{\mathrm{L}}^{-}e^{\eta_{\mathrm{L}}^{+}\delta} & k_{\mathrm{out}}^{\mathrm{R}}D\eta_{\mathrm{L}}^{+}e^{\eta_{\mathrm{L}}^{-}\delta} \\
k_{\mathrm{out}}^{\mathrm{R}}k_{\mathrm{out}}^{\mathrm{L}}\gamma\tau & 0 & -k_{\mathrm{out}}^{\mathrm{R}}D\eta_{\mathrm{L}}^{-} & -k_{\mathrm{out}}^{\mathrm{R}}D\eta_{\mathrm{L}}^{+} \\
k_{\mathrm{out}}^{\mathrm{R}}k_{\mathrm{out}}^{\mathrm{L}}\gamma\tau & 0 & -k_{\mathrm{out}}^{\mathrm{R}}D\eta_{\mathrm{L}}^{-}e^{\eta_{\mathrm{L}}^{+}\delta} & -k_{\mathrm{out}}^{\mathrm{R}}D\eta_{\mathrm{L}}^{+}e^{\eta_{\mathrm{L}}^{-}\delta} \\
k_{\mathrm{in}}^{\mathrm{R}}k_{\mathrm{out}}^{\mathrm{L}}-k_{\mathrm{out}}^{\mathrm{R}}k_{\mathrm{in}}^{\mathrm{L}} & k_{\mathrm{in}}^{\mathrm{R}}k_{\mathrm{out}}^{\mathrm{L}}e^{\xi\delta}-k_{\mathrm{out}}^{\mathrm{R}}k_{\mathrm{in}}^{\mathrm{L}} & -k_{\mathrm{in}}^{\mathrm{R}}e^{\eta_{\mathrm{L}}^{+}\delta}-k_{\mathrm{out}}^{\mathrm{R}} & -k_{\mathrm{in}}^{\mathrm{R}}e^{\eta_{\mathrm{L}}^{-}\delta}-k_{\mathrm{out}}^{\mathrm{R}} \\
0 & k_{\mathrm{in}}^{\mathrm{R}}k_{\mathrm{in}}^{\mathrm{L}}(1-e^{\xi\delta}) & k_{\mathrm{in}}^{\mathrm{R}}(1-e^{\eta_{\mathrm{L}}^{+}\delta}) & k_{\mathrm{in}}^{\mathrm{R}}(1-e^{\eta_{\mathrm{L}}^{-}\delta}) \\
0 & \xi k_{\mathrm{in}}^{\mathrm{R}}k_{\mathrm{in}}^{\mathrm{L}}(1-e^{\xi\delta}) & k_{\mathrm{in}}^{\mathrm{R}}\eta_{\mathrm{L}}^{+}(1-e^{\eta_{\mathrm{L}}^{+}\delta}) & k_{\mathrm{in}}^{\mathrm{R}}\eta_{\mathrm{L}}^{-}(1-e^{\eta_{\mathrm{L}}^{-}\delta}) \\
\delta & (e^{\xi\delta}-1)/\xi & 0 & 0
\end{bmatrix}$$

$$\begin{bmatrix}
k_{\mathrm{out}}^{\mathrm{L}}D\eta_{\mathrm{R}}^{-} & k_{\mathrm{out}}^{\mathrm{L}}D\eta_{\mathrm{R}}^{+} & -D\eta_{\mathrm{LR}}^{-} & -D\eta_{\mathrm{LR}}^{+} \\
-k_{\mathrm{in}}^{\mathrm{L}}D\eta_{\mathrm{R}}^{-}e^{\eta_{\mathrm{R}}^{+}\delta} & -k_{\mathrm{in}}^{\mathrm{L}}D\eta_{\mathrm{R}}^{+}e^{\eta_{\mathrm{R}}^{-}\delta} & -D\eta_{\mathrm{LR}}^{-}e^{\eta_{\mathrm{LR}}^{+}\delta} & -D\eta_{\mathrm{LR}}^{+}e^{\eta_{\mathrm{LR}}^{-}\delta} \\
-k_{\mathrm{out}}^{\mathrm{L}}D\eta_{\mathrm{R}}^{-} & -k_{\mathrm{out}}^{\mathrm{L}}D\eta_{\mathrm{R}}^{+} & D\eta_{\mathrm{LR}}^{-} & D\eta_{\mathrm{LR}}^{+} \\
-k_{\mathrm{out}}^{\mathrm{L}}D\eta_{\mathrm{R}}^{-}e^{\eta_{\mathrm{R}}^{+}\delta} & -k_{\mathrm{out}}^{\mathrm{L}}D\eta_{\mathrm{R}}^{+}e^{\eta_{\mathrm{R}}^{-}\delta} & D\eta_{\mathrm{LR}}^{-}e^{\eta_{\mathrm{LR}}^{+}\delta} & D\eta_{\mathrm{LR}}^{+}e^{\eta_{\mathrm{LR}}^{-}\delta} \\
k_{\mathrm{out}}^{\mathrm{L}}e^{\eta_{\mathrm{R}}^{+}\delta}+k_{\mathrm{in}}^{\mathrm{L}} & k_{\mathrm{out}}^{\mathrm{L}}e^{\eta_{\mathrm{R}}^{-}\delta}+k_{\mathrm{in}}^{\mathrm{L}} & 1-e^{\eta_{\mathrm{LR}}^{+}\delta} & 1-e^{\eta_{\mathrm{LR}}^{-}\delta} \\
k_{\mathrm{in}}^{\mathrm{L}}(1-e^{\eta_{\mathrm{R}}^{+}\delta}) & k_{\mathrm{in}}^{\mathrm{L}}(1-e^{\eta_{\mathrm{R}}^{-}\delta}) & 1-e^{\eta_{\mathrm{LR}}^{+}\delta} & 1-e^{\eta_{\mathrm{LR}}^{-}\delta} \\
k_{\mathrm{in}}^{\mathrm{L}}\eta_{\mathrm{R}}^{+}(1-e^{\eta_{\mathrm{R}}^{+}\delta}) & k_{\mathrm{in}}^{\mathrm{L}}\eta_{\mathrm{R}}^{-}(1-e^{\eta_{\mathrm{R}}^{-}\delta}) & \eta_{\mathrm{LR}}^{+}(1-e^{\eta_{\mathrm{LR}}^{+}\delta}) & \eta_{\mathrm{LR}}^{-}(1-e^{\eta_{\mathrm{LR}}^{-}\delta}) \\
0 & 0 & 0 & 0
\end{bmatrix}. \tag{36}$$

We find useful formulas for the probability and the flow in state i. For the probabilities, the following relations hold in the steady state:

$$0=-(k_{\mathrm{in}}^{\mathrm{R}}+k_{\mathrm{in}}^{\mathrm{L}})\overline{p_{\mathrm{E}}}+k_{\mathrm{out}}^{\mathrm{R}}\overline{p_{\mathrm{R}}}+k_{\mathrm{out}}^{\mathrm{L}}\overline{p_{\mathrm{L}}}, \tag{37}$$

$$\Pi_{\mathrm{R}}(\delta)=k_{\mathrm{in}}^{\mathrm{R}}\overline{p_{\mathrm{E}}}-(k_{\mathrm{out}}^{\mathrm{R}}+k_{\mathrm{in}}^{\mathrm{L}})\overline{p_{\mathrm{R}}}+k_{\mathrm{out}}^{\mathrm{L}}\overline{p_{\mathrm{F}}}, \tag{38}$$

$$-\Pi_{\mathrm{R}}(\delta)=k_{\mathrm{in}}^{\mathrm{L}}\overline{p_{\mathrm{E}}}-(k_{\mathrm{in}}^{\mathrm{R}}+k_{\mathrm{out}}^{\mathrm{L}})\overline{p_{\mathrm{L}}}+k_{\mathrm{out}}^{\mathrm{R}}\overline{p_{\mathrm{F}}}, \tag{39}$$

$$0=k_{\mathrm{in}}^{\mathrm{L}}\overline{p_{\mathrm{R}}}+k_{\mathrm{in}}^{\mathrm{R}}\overline{p_{\mathrm{L}}}-(k_{\mathrm{out}}^{\mathrm{R}}+k_{\mathrm{out}}^{\mathrm{L}})\overline{p_{\mathrm{F}}}, \tag{40}$$

where

$$\overline{p_i}=\int_0^{\delta} dx p_i(x). \tag{41}$$

The relations above are obtained by integrating Eq. (4) over x and using the boundary conditions (7)–(10). For the flow of probability, the following relation holds:

$$\overline{\Pi_i} \equiv \int_0^\delta dx \Pi_i(x) = \gamma\tau\overline{p_i(x)} + D[p_i(0) - p_i(\delta)], \tag{42}$$

which are obtained by integrating Eq. (5) with respect to x.

Let us now derive formulas for the observables; the average rotation velocity $\langle v \rangle$, the proton translocation rate $N(\mathrm{H}^+)$, and the efficiency of energy transduction. The average rotation velocity $\langle v \rangle$ is given by the total sum of the integrated flow of probability,

$$\langle v \rangle = \sum_{i=E,R,L,F} \overline{\Pi}_i. \tag{43}$$

Using Eq. (28), we obtain

$$\langle v \rangle = \gamma\tau\delta C_1 (k_{\mathrm{in}}^{\mathrm{L}} + k_{\mathrm{out}}^{\mathrm{L}})(k_{\mathrm{in}}^{\mathrm{R}} + k_{\mathrm{out}}^{\mathrm{R}}). \tag{44}$$

The proton translocation rate $N(\mathrm{H}^+)$ is given as follows: A proton goes out from the left binding site to the cytoplasma when the state L becomes E or F becomes R. When E becomes L or R becomes F, a proton comes back to the left binding site. So the flow of the left binding site J_{L} is defined as

$$J_{\mathrm{L}} = k_{\mathrm{out}}^{\mathrm{L}}\overline{p}_{\mathrm{L}} - k_{\mathrm{in}}^{\mathrm{L}}\overline{p}_{\mathrm{E}} + k_{\mathrm{out}}^{\mathrm{L}}\overline{p}_{\mathrm{F}} - k_{\mathrm{in}}^{\mathrm{L}}\overline{p}_{\mathrm{R}}. \tag{45}$$

In a similar way, the flow of the right binding site is written as

$$J_{\mathrm{R}} = -k_{\mathrm{out}}^{\mathrm{R}}\overline{p}_{\mathrm{R}} + k_{\mathrm{in}}^{\mathrm{R}}\overline{p}_{\mathrm{E}} - k_{\mathrm{out}}^{\mathrm{R}}\overline{p}_{\mathrm{F}} + k_{\mathrm{in}}^{\mathrm{R}}\overline{p}_{\mathrm{L}}. \tag{46}$$

For the system to be in a steady state, J_{L} and J_{R} must be equivalent and we obtain

$$\begin{aligned} N(\mathrm{H}^+) &= J_{\mathrm{L}} \\ &= J_{\mathrm{R}} \\ &= \tfrac{1}{2}\{J_{\mathrm{L}} + J_{\mathrm{R}}\} \\ &= \tfrac{1}{2}[(k_{\mathrm{in}}^{\mathrm{R}} - k_{\mathrm{in}}^{\mathrm{L}})\overline{p}_{\mathrm{E}} - (k_{\mathrm{out}}^{\mathrm{R}} + k_{\mathrm{in}}^{\mathrm{L}})\overline{p}_{\mathrm{R}} + (k_{\mathrm{in}}^{\mathrm{R}} + k_{\mathrm{out}}^{\mathrm{L}})\overline{p}_{\mathrm{L}} \\ &\quad + (k_{\mathrm{out}}^{\mathrm{L}} - k_{\mathrm{out}}^{\mathrm{R}})\overline{p}_{\mathrm{F}}]. \end{aligned} \tag{47}$$

Using Eqs. (38) and (39), we find that this $N(\mathrm{H}^+)$ is simply given by $\Pi_R(\delta)$ and evaluated as

$$\begin{aligned} N(\mathrm{H}^+) &= \tfrac{1}{2}[\text{Eq. (38)} - \text{Eq. (39)}] \\ &= \Pi_{\mathrm{R}}(\delta)[= \Pi_{\mathrm{L}}(0)] \\ &= k_{\mathrm{in}}^{\mathrm{R}} k_{\mathrm{out}}^{\mathrm{L}} C_1 \gamma\tau - k_{\mathrm{in}}^{\mathrm{R}}(C_3 D \eta_{\mathrm{L}}^- e^{\eta_{\mathrm{L}}^+\delta} + C_4 D \eta_{\mathrm{L}}^+ e^{\eta_{\mathrm{L}}^-\delta}) \\ &\quad + k_{\mathrm{out}}^{\mathrm{L}}(C_5 D \eta_{\mathrm{R}}^- e^{\eta_{\mathrm{R}}^+\delta} + C_6 D \eta_{\mathrm{R}}^+ e^{\eta_{\mathrm{R}}^-\delta}) \\ &\quad - (C_7 D \eta_{\mathrm{LR}}^- e^{\eta_{\mathrm{LR}}^+\delta} + C_8 D \eta_{\mathrm{LR}}^+ e^{\eta_{\mathrm{LR}}^-\delta}). \end{aligned} \tag{48}$$

Finally, we define the efficiency of energy transduction as follows:

$$e \equiv \frac{-\tau\langle v \rangle}{\Delta G N(\mathrm{H}^+)}. \tag{49}$$

This definition coincides with that given in Ref. [18].

III. RESULTS

We investigate the dependence of the quantities $\langle v \rangle$, $N(\mathrm{H}^+)$, and e on the transition rate $\hat{\mathbf{K}}$ using the above analytical solution. Parameters used for calculation are, according to Ref. [19], $D = 2\times10^4$ rad^2 sec^{-1}, $k_{\mathrm{B}}T = 4$ pN nm, $\gamma = 5\times10^3$ rad^2 sec^{-1} pN^{-1} nm^{-1}, and $\tau = -40$ pN nm. The transition rates are given as

$$\begin{bmatrix} k_{\mathrm{in}}^{\mathrm{R}} \\ k_{\mathrm{in}}^{\mathrm{L}} \\ k_{\mathrm{out}}^{\mathrm{R}} \\ k_{\mathrm{out}}^{\mathrm{L}} \end{bmatrix} = 10^K \begin{bmatrix} 10^{-pH_{\mathrm{A}}} e^{\phi/k_{\mathrm{B}}T} \\ 10^{-pH_{\mathrm{B}}} e^{\phi/k_{\mathrm{B}}T} \\ 10^{-pK_a} e^{-V/2k_{\mathrm{B}}T} \\ 10^{-pK_a} e^{V/2k_{\mathrm{B}}T} \end{bmatrix}, \tag{50}$$

where $pH_{\mathrm{A}} = 7.0$ and $pH_{\mathrm{B}} = 8.4$ are the proton concentrations of each side (A, acidic; B, basic), pK_a is the acidity of proton binding site, $\phi = 2.3k_{\mathrm{B}}T$ is the surface effect, and $V = 5.6k_{\mathrm{B}}T$ is the membrane potential (the proton binding site is assumed to be in the middle of the membrane). The overall factor 10^K means the proton absorption rate of the path. Since it depends on the proton diffusion coefficient and the surface area of the channel, we assume that this factor is common for all transition rates. Variation of K is also regarded as varying pH of each side and pK_a, preserving the differences of each other.

We plot the dependence of $\langle v \rangle$, $N(\mathrm{H}^+)$, and e on K in Figs. 3–5. For the rotation velocity $\langle v \rangle$, no qualitative difference dependent on pK_a is found. There is almost no rotation in the desirable direction when the chemical reaction rate is low (namely, when K is small). Then the velocity monotonically increases as K increases and saturates when the reaction is very fast. For the proton translocation rate, $N(\mathrm{H}^+)$, a qualitative difference dependent on pK_a is found though almost no translocation is observed during small K in both cases. For $pK_a = 5.5$, $N(\mathrm{H}^+)$ increases monotonically. On the other hand, for $pK_a = 4.5$, while it increases monotonically also, there exists a region where the increase becomes very slow ($K \sim 10$–12). In both pK_a's, $N(\mathrm{H}^+)$ diverges as $10^{K/2}$ when K becomes large enough. The efficiency e reflects the above results of $\langle v \rangle$ and $N(\mathrm{H}^+)$. In both pK_a's, it increases as K increases at first. Then it reaches a peak value (at $K \sim 12$ for $pK_a = 5.5$ and at $K \sim 13$ for $pK_a = 4.5$) and decreases monotonically afterward. The efficiency goes to zero as K diverges reflecting the fact that

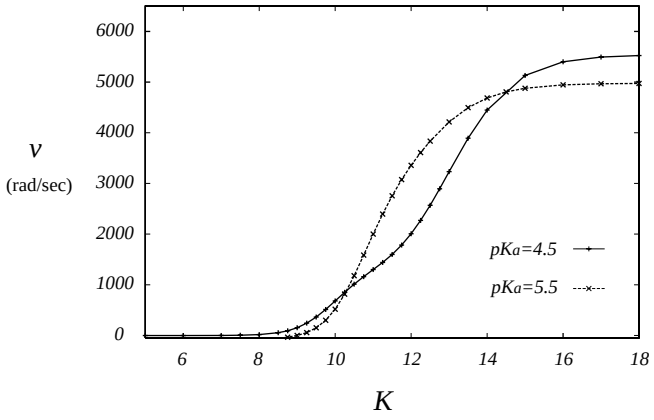

FIG. 3. The rotation velocity $\langle v \rangle$. K of the abscissa is that of Eq. (50). The solid line with +'s is the plot for $pK_a=4.5$ and the broken line with ×'s is for $pK_a=5.5$. There is almost no rotation in the region of small K. The faster the chemical reaction, the more this quantity increases monotonically and saturates finally.

$\langle v \rangle$ converges to the finite value but $N(\mathrm{H}^+)$ diverges for large K. Note that the peak value of the efficiency for $pK_a=4.5$ is enhanced and is about 25% larger than that for $pK_a=5.5$. This comes from the slow increase of $N(\mathrm{H}^+)$ for $pK_a=4.5$ described above.

Inferring from the forms of Eqs. (23)–(26), the key to account for these results are thought to be the inequalities between the chemical reaction rates k_j^i's ($i=E,R,L,F$ and $j=$in, out) and the reciprocal of the relaxation time of this convection-diffusion system, $(\gamma\tau)^2/D$. The inequalities between k_j^i's for $pK_a=5.5$ are different to those for $pK_a=4.5$. For $pK_a=5.5$, the inequalities are $k_{\mathrm{out}}^{\mathrm{L}} > k_{\mathrm{in}}^{\mathrm{R}} > k_{\mathrm{out}}^{\mathrm{R}} > k_{\mathrm{in}}^{\mathrm{L}}$, while for $pK_a=4.5$, $k_{\mathrm{out}}^{\mathrm{L}} > k_{\mathrm{out}}^{\mathrm{R}} > k_{\mathrm{in}}^{\mathrm{R}} > k_{\mathrm{in}}^{\mathrm{L}}$. Under the parameters used here, which are plausible in living body, only the above two sets of inequalities are possible for the model to work well. Note that the inequalities $k_{\mathrm{in}}^{\mathrm{R}} > k_{\mathrm{in}}^{\mathrm{L}}$ and

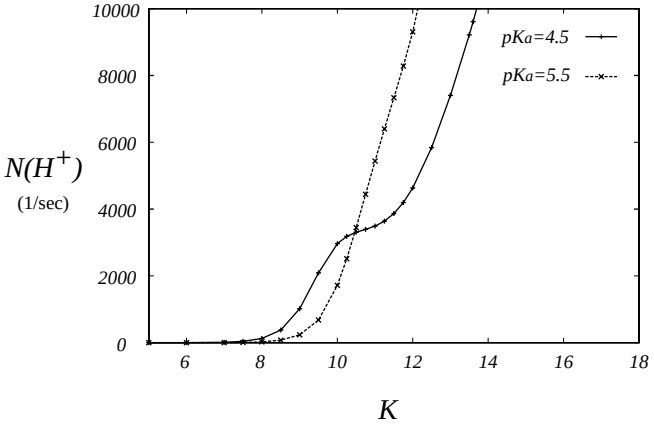

FIG. 4. The proton translocation rate $N(\mathrm{H}^+)$. The solid line with +'s is the plot for $pK_a=4.5$ and the broken line with ×'s is for $pK_a=5.5$. There is almost no translocation observed for small K in both cases. For $pK_a=4.5$, there exists a region where the increase becomes very slow ($K\sim 10-12$). At large K, it diverges as $10^{K/2}$.

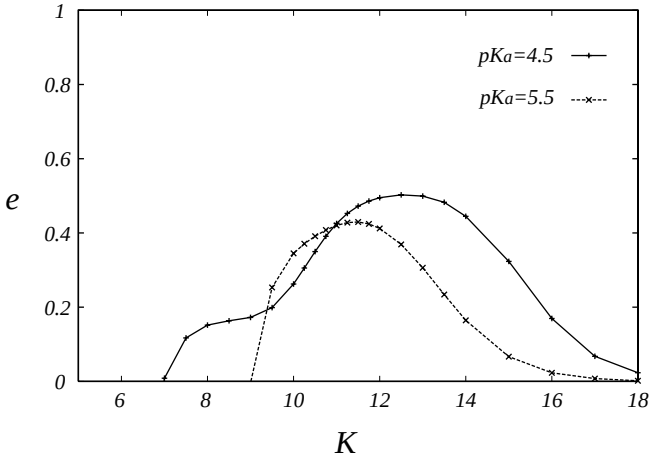

FIG. 5. The transduction efficiency e. The solid line with +'s is the plot for $pK_a=4.5$ and the broken line with ×'s is for $pK_a=5.5$. It has a peak at $K\sim 13$ and $e\sim 0.5$ for $pK_a=4.5$, and $K\sim 12$ and $e\sim 0.4$ for $pK_a=5.5$. For large K, it converges to 0 reflecting the fact that $\langle v \rangle$ converges and $N(\mathrm{H}^+)$ diverges.

$k_{\mathrm{out}}^{\mathrm{L}} > k_{\mathrm{out}}^{\mathrm{R}}$ hold since the proton concentration in the acidic side are higher than that in the basic side and the difference makes the transmembrane electrostatic potential, and also that $k_{\mathrm{out}}^{\mathrm{L}} > k_{\mathrm{in}}^{\mathrm{L}}$ is required for the motor not to diffuse leftward by the load torque τ from the F_1 part.

While the above two sets of inequalities between k_j^i's do not depend on K, the inequalities between $(\gamma\tau)^2/D$ and k_j^i's do depend on K. And k_j^i's which are larger than $(\gamma\tau)^2/D$ are relevant to the dynamics of the system. When K is small enough, $(\gamma\tau)^2/D$ is the largest among them. Thus all the transition rates between the states are neglected, so the motor does not work well. As K increases, k_j^i's also increase, and when $K\approx 9.5$ for $pK_a=4.5$ and $K\approx 10.5$ for $pK_a=5.5$, the largest rate $k_{\mathrm{out}}^{\mathrm{L}}$ becomes comparable to $(\gamma\tau)^2/D$. A proton in the left channel can dissociate before diffusion and state R is created. Thus $\overline{\Pi}_{\mathrm{R}}$ increases and is the largest among $\overline{\Pi}_i$'s in this region of K.

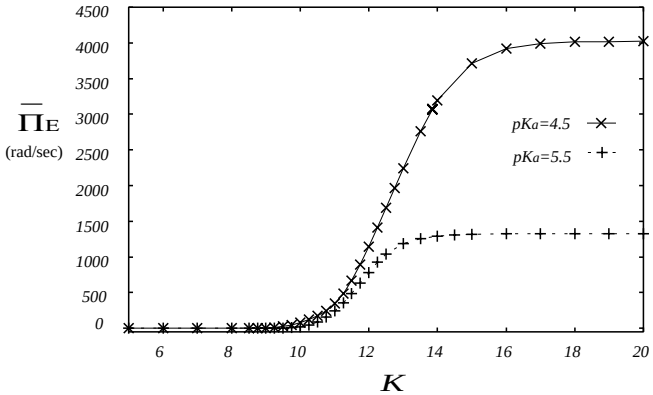

FIG. 6. The integrated flow of state E. The solid line with ×'s is the plot for $pK_a=4.5$ and the dotted line with +'s is for $pK_a=5.5$. It increases monotonically both for $pK_a=4.5$ and 5.5.

Next, for $pK_a=4.5$, $k_{\rm out}^{\rm R}$ becomes comparable to $(\gamma\tau)^2/D$ when $K\approx 12$. Near this region of K, a proton in the right channel in state R can dissociate before diffusion, so state R becomes state E. Thus $\overline{\Pi}_R$ decreases until $\overline{\Pi}_E$ becomes larger than $\overline{\Pi}_R$. As a result, the increase of $N(\mathrm{H}^+)$ $[=\overline{\Pi}_R(\delta)]$ is suppressed in this region, but not of $\langle v\rangle$ because the increase of $\overline{\Pi}_E$ cancels out the decrease of $\overline{\Pi}_R$ (see Figs. 3 and 4). On the other hand, for $pK_a=5.5$, $\overline{\Pi}_R$ continues to increase since $k_{\rm in}^{\rm R}$ is larger than $k_{\rm out}^{\rm R}$. Thus $N(H^+)$ and $\langle v\rangle$ increase monotonically.

At last, when $K\gtrsim 16$, all the transition rates become sufficiently greater than $(\gamma\tau)^2/D$, so the matrix $\hat{\mathbf{M}}$ is reduced to

$\hat{\mathbf{M}}$

$$\rightarrow\begin{bmatrix}
k_{\rm in}^{\rm R}k_{\rm out}^{\rm L}\gamma\tau & 0 & 0 & -k_{\rm in}^{\rm R}D\eta_{\rm L} & 0 & k_{\rm out}^{\rm L}D\eta_{\rm R} & 0 & -D\eta_{\rm LR}\\
k_{\rm out}^{\rm R}k_{\rm in}^{\rm L}\gamma\tau & 0 & -k_{\rm out}^{\rm R}D\eta_{\rm L}e^{\eta_{\rm L}\delta} & 0 & k_{\rm in}^{\rm L}D\eta_{\rm R}e^{\eta_{\rm R}\delta} & 0 & -D\eta_{\rm LR}e^{\eta_{\rm LR}\delta} & 0\\
k_{\rm out}^{\rm R}k_{\rm out}^{\rm L}\gamma\tau & 0 & 0 & -k_{\rm out}^{\rm R}D\eta_{\rm L} & 0 & -k_{\rm out}^{\rm L}D\eta_{\rm R} & 0 & D\eta_{\rm LR}\\
k_{\rm out}^{\rm R}k_{\rm out}^{\rm L}\gamma\tau & 0 & k_{\rm out}^{\rm R}D\eta_{\rm L}e^{\eta_{\rm L}\delta} & 0 & k_{\rm out}^{\rm L}D\eta_{\rm R}e^{\eta_{\rm R}\delta} & 0 & D\eta_{\rm LR}e^{\eta_{\rm LR}\delta} & 0\\
k_{\rm in}^{\rm R}k_{\rm out}^{\rm L}-k_{\rm out}^{\rm R}k_{\rm in}^{\rm L} & k_{\rm in}^{\rm R}k_{\rm out}^{\rm L}e^{\xi\delta}-k_{\rm out}^{\rm R}k_{\rm in}^{\rm L} & -k_{\rm in}^{\rm R}e^{\eta_{\rm L}\delta} & -k_{\rm out}^{\rm R} & k_{\rm out}^{\rm L}e^{\eta_{\rm R}\delta} & k_{\rm in}^{\rm L} & -e^{\eta_{\rm LR}\delta} & 1\\
0 & k_{\rm in}^{\rm R}k_{\rm in}^{\rm L}(1-e^{\xi\delta}) & -k_{\rm in}^{\rm R}e^{\eta_{\rm L}\delta} & k_{\rm in}^{\rm R} & -k_{\rm in}^{\rm L}e^{\eta_{\rm R}\delta} & k_{\rm in}^{\rm L} & -e^{\eta_{\rm LR}\delta} & 1\\
0 & \xi k_{\rm in}^{\rm R}k_{\rm in}^{\rm L}(1-e^{\xi\delta}) & -k_{\rm in}^{\rm R}\eta_{\rm L}e^{\eta_{\rm L}\delta} & -k_{\rm in}^{\rm R}\eta_{\rm L} & -k_{\rm in}^{\rm L}\eta_{\rm R}e^{\eta_{\rm R}\delta} & -k_{\rm in}^{\rm L}\eta_{\rm R} & -\eta_{\rm LR}^{+}e^{\eta_{\rm LR}\delta}) & -\eta_{\rm LR}\\
\delta & (e^{\xi\delta}-1)/\xi & 0 & 0 & 0 & 0 & 0 & 0
\end{bmatrix}, \tag{51}$$

where

$$\eta_{\rm L}=\sqrt{(k_{\rm in}^{\rm L}+k_{\rm out}^{\rm L})/D}, \tag{52}$$

$$\eta_{\rm R}=\sqrt{(k_{\rm in}^{\rm R}+k_{\rm out}^{\rm R})/D}, \tag{53}$$

and

$$\eta_{\rm LR}=\sqrt{(k_{\rm in}^{\rm L}+k_{\rm out}^{\rm L}+k_{\rm in}^{\rm R}+k_{\rm out}^{\rm R})/D}. \tag{54}$$

(In this limit, $\eta_i^{\pm}\rightarrow\pm\eta_i$.) From this, it is easily found that $C_{1-2}=O(10^{-2K})$, $C_{3-6}=O(10^{-K})$, and $C_{7-8}=O(1)$, so $\langle v\rangle$ converges when K diverges. The convergent value of $\langle v\rangle_{K\rightarrow\infty}$ is given by

$$\langle v\rangle_{K\rightarrow\infty}=\frac{\gamma^2\tau^2\delta[-bc+a\{e^{\gamma\tau\delta/D}+b(e^{\gamma\tau\delta/D}-1)\}]}{bc\{D(e^{\gamma\tau\delta/D}-1)-\gamma\tau\delta\}+a[D-De^{\gamma\tau\delta/D}+\gamma\tau\delta\{e^{\gamma\tau\delta/D}+b(e^{\gamma\tau\delta/D}-1)\}]}, \tag{55}$$

where $a=k_{\rm in}^{\rm R}/k_{\rm out}^{\rm L}$, $b=k_{\rm in}^{\rm L}/k_{\rm out}^{\rm L}$, $c=k_{\rm out}^{\rm R}/k_{\rm out}^{\rm L}$. Comparing Eq. (48) with Eq. (44), it is also found that $N(\mathrm{H}^+)=O(10^{K/2})$. The divergent behavior of $N(\mathrm{H}^+)$ is consistent with Fig. 4.

We show the integrated flows of probability for states E and R, $\overline{\Pi}_E$ and $\overline{\Pi}_R$, in Figs. 6 and 7. Their behaviors are consistent with the above explanations. We also see that $\overline{\Pi}_{\rm F}$ and $\overline{\Pi}_{\rm L}$ are much smaller than $\overline{\Pi}_{\rm E}$ and $\overline{\Pi}_{\rm R}$ under the above two sets of inequalities ($k_{\rm out}^{\rm L}>k_{\rm in}^{\rm R}>k_{\rm out}^{\rm R}>k_{\rm in}^{\rm L}$ and $k_{\rm out}^{\rm L}>k_{\rm out}^{\rm R}>k_{\rm in}^{\rm R}>k_{\rm in}^{\rm L}$) (see Fig. 8). Thus the qualitative behavior of $\langle v\rangle$ and $N(\mathrm{H}^+)$ is determined by only the states E and R. This is also consistent with the above explanation which neglects the states L and F.

IV. SUMMARY AND DISCUSSION

We have investigated the rotatory molecular motor using simply the biased diffusion model. The model depends on four chemical reaction rates $k_{\rm L}^{\rm in}$, $k_{\rm L}^{\rm out}$, $k_{\rm R}^{\rm in}$, $k_{\rm R}^{\rm out}$, the diffusion and the friction constants of the motor, D, γ, and the load torque, τ. We have solved the model analytically, and examined the relation between these chemical reaction rates and

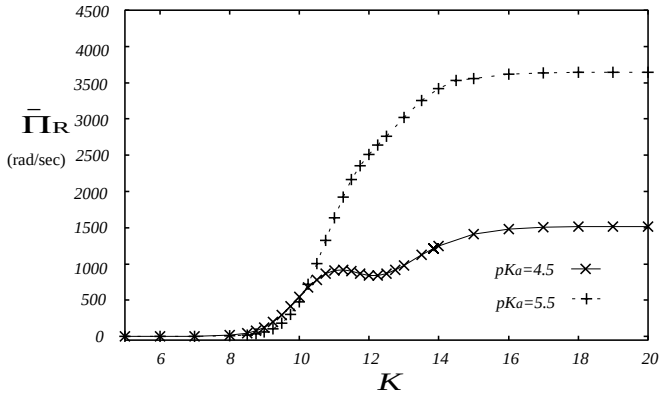

FIG. 7. The integrated flow of state *R*. The solid line with ×'s is the plot for $pK_a=4.5$ and the dotted line with +'s is for $pK_a=5.5$. For $pK_a=5.5$, it increases monotonically. But for $pK_a=4.5$, there is a region where it decreases.

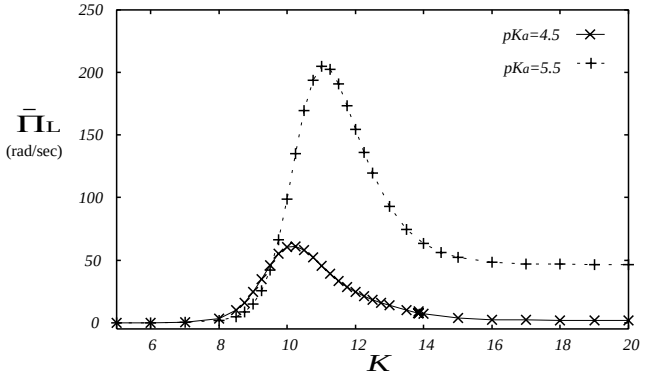

FIG. 8. The integrated flow of state *L*. The solid line with ×'s is the plot for $pK_a=4.5$ and the dotted line with +'s is for $pK_a=5.5$. It has a peak for $K\approx 11$ for $pK_a=5.5$ and $K\approx 10$ for $pK_a=4.5$.

the physical quantities, such as the rotational velocity, the proton translocation rate, and the efficiency of the energy transduction. It is found that below such value of K as $k_{\mathrm{out}}^{\mathrm{L}}$, the largest among k_j^i's, becomes comparable with $(\gamma\tau)^2/D$, both $\langle v\rangle$ and $N(\mathrm{H}^+)$ are very low so this model does not work well and results in bad efficiency, and that there exists an optimal value for the chemical reaction to maximize the efficiency of the energy transduction. We also found that when the inequalities $k_{\mathrm{out}}^{\mathrm{L}}>(\gamma\tau)^2/D>k_{\mathrm{out}}^{\mathrm{R}}>k_{\mathrm{in}}^{\mathrm{R}}>k_{\mathrm{in}}^{\mathrm{L}}$ hold, the increase of the proton translocation can become very slow and the efficiency of the motor is enhanced. This efficiency enhanced mechanism is naturally explained from this set of inequalities.

This model is based on the diffusion process like the thermal ratchet model for linear molecular motors [21], so that the efficiency enhancement mechanism above may give a clue to examine whether diffusion process dominates the motion of molecular motor essentially or not. The inequality is controlled by the dissociation constant of the proton binding sites, pK_a, the proton concentration of both sides of the membrane, the proton diffusion constant, etc.

The efficiency of this model is still not high compared with that reported in Ref. [12]. There are some possibilities which can explain this.

(1) The definition of efficiency may still be vague and controversial. In Ref. [12], the authors adapted a different definition of the efficiency from ours. Our definition coincides with that in Ref. [18], where the energetics of the Langevin equations and the Fokker-Planck equations are carefully analyzed.

(2) There may be a necessity to reconsider the several relations between physical quantities which we assume to be appropriate near equilibrium, such as the Einstein's relation, since molecular motor is a nonequilibrium system far from equilibrium.

(3) There may be another mechanism which enhances the efficiency. For instance, an electrostatic interaction between residues is discussed in Ref. [19]. Furthermore, experimentally conformational change of the motor protein during motion is reported [22]. It is important to construct a model which gets along with this experimental result. These may be the key to account for the high efficiency of energy transduction of molecular motors.

[1] J. Howard, *Mechanics of Motor Proteins and the Cytoskelton* (Sinauer, Sunderland, MA, 2001).
[2] R.D. Vale and R.A. Milligan, Science **288**, 88 (2000).
[3] H. Lodish, A. Berk, S.L. Zipurski, P. Matsudaira, D. Baltimore, and J. Darnell, *Molecular Cell Biology*, 4th ed. (Freeman, New York, 1999).
[4] R.L. Cross and T.M. Duncan, J. Bioenerg. Biomembr. **28**, 403 (1996).
[5] S.B. Vik and B.J. Antonio, J. Biol. Chem. **269**, 30 364 (1994).
[6] D. Subbert, S. Engelbrecht, and W. Junge, Nature (London) **381**, 623 (1996).
[7] D. Stock, A.G.W. Leslie, and J.E. Walker, Science **286**, 1700 (1999).
[8] Y. Sambongi *et al.*, Science **286**, 1722 (1999).
[9] S.P. Tsunoda, R. Aggeler, M. Yoshida, and R.A. Capaldi, Proc. Natl. Acad. Sci. U.S.A. **98**, 898 (2001).
[10] M.L. Hutcheon, T.M. Duncan, H. Ngai, and R.L. Cross, Proc. Natl. Acad. Sci. U.S.A. **98**, 8519 (2001).
[11] P.D. Boyer, Biochim. Biophys. Acta **1140**, 215 (1993); **1458**, 252 (2000).
[12] H. Noji, R. Yasuda, M. Yoshida, and K. Kinoshita, Nature (London) **386**, 299 (1997).
[13] T.M. Duncan *et al.*, Proc. Natl. Acad. Sci. U.S.A. **92**, 10 964 (1995).
[14] Y. Zhou, T.M. Duncan, and R.J. Cross, Proc. Natl. Acad. Sci. U.S.A. **94**, 10 583 (1997).
[15] J.P. Abrahams *et al.*, Nature (London) **370**, 621 (1994).

[16] T. Matsui *et al.*, J. Biol. Chem. **272**, 8215 (1997).
[17] H. Wang and G. Oster, Nature (London) **396**, 279 (1998), and supplementary material.
[18] K. Sekimoto, J. Phys. Soc. Jpn. **66**, 1234 (1997).
[19] T. Elston, H. Wang, and G. Oster, Nature (London) **391**, 510 (1998), and supplementary material.
[20] W. Junge, H. Lill, and S. Engelbrecht, Trends Biochem. Sci. **22**, 420 (1997).
[21] F. Jülicher, A. Ajdari, and J. Prost, Rev. Mod. Phys. **69**, 1269 (1997).
[22] V.K. Rastogi and M.E. Garvin, Nature (London) **402**, 263 (1999).